CHEMISTRY
A EUROPEAN JOURNAL

DOI: 10.1002/chem.200701227

# Autonomous Movement of Silica and Glass Micro-Objects Based on a Catalytic Molecular Propulsion System

**Christoph Stock, Nicolas Heureux, Wesley R. Browne, and Ben L. Feringa*[a]**

**Abstract:** A general approach for the easy functionalization of bare silica and glass surfaces with a synthetic manganese catalyst is reported. Decomposition of $H_2O_2$ by this dinuclear metallic center into $H_2O$ and $O_2$ induced autonomous movement of silica microparticles and glass micro-sized fibers. Although several mechanisms have been proposed to rationalise movement of particles driven by $H_2O_2$ decomposition to $O_2$ and water (recoil from $O_2$ bubbles,[36,45] interfacial tension gradient[37–42]), it is apparent in the present system that ballistic movement is due to the growth of $O_2$ bubbles.

**Keywords:** autonomous movement · manganese · microparticles · molecular motor · surface analysis

## Introduction

Controlled movement is one of the most fascinating features of living cells.[1] However, locomotion on the micro- and nanoscale through a fluid environment, in synthetic systems, remains one of the major challenges confronting nanotechnology today.[2–12] The bottom-up construction of molecular-level motors has brought the prospect of synthetic molecular based mechanical machines within sight. Artificial molecular systems constructed in order to mimic aspects of mechanical function include shutlles,[13–17] rotors,[18–21] muscles,[22–24] switches,[25–28] elevators[29,30] and motors.[31–35]

An attractive approach to apply chemical transformations, that is, using a chemical fuel, to induce translational motion is based on a seminal contribution by Whitesides and co-workers.[36] Rotational and translational movement of millimeter and micrometer-sized objects[37–41] has been achieved using bimetallic systems and $H_2O_2$ as a fuel with proposed propulsion mechanisms including oxygen bubble formation, change in surface tension or oxygen gradients.[42] Propulsion of conductive carbon fibers, using a bio-electrocatalyst, able to decompose glucose and oxygen into gluconolactone and water, was reported by Mano and Heller.[43] More recently, self-propulsion of millimeter-sized semiconductor diodes, through an electric field, was reported by the group of Velev.[44] In a molecular approach to autonomous movement, we recently reported a synthetic oxygen evolving complex as the catalyst for a micro-scale propulsion system.[45] In our design, the micro-sized object, for instance a silica microparticle (40–80 μm), is linked, via a short spacer, to a metal complex, able to catalyze $H_2O_2$ disproportionation at a molecular level (Scheme 1).

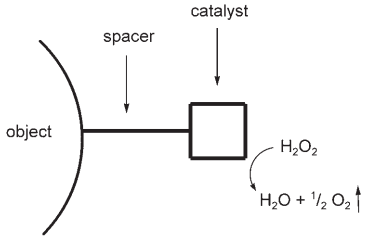


Scheme 1. Design of a system propelled by a catalytic molecular motor.

The use of a molecular catalytic complex was found to be of a considerable advantage, as it can be easily modified, tether length can be adjusted, and local catalyst density is controllable. Moreover, we considered that a molecular

[a] Dr. C. Stock, Dr. N. Heureux, Dr. W. R. Browne, Prof. Dr. B. L. Feringa
Organic Chemistry Laboratories
Stratingh Institute for Chemistry & Zernike Institute for Advanced Materials
University of Groningen, Nijenborgh 4
9747 AG Groningen (The Netherlands)
Fax: (+31) 50-363-4296
E-mail: b.l.feringa@rug.nl

Supporting information for this article is available on the WWW under http://www.chemeurj.org/ or from the author: Movies of autonomous movement of a silica microparticle and of glass fibers.

system would be easily adaptable on different kinds of materials, giving the extensive background in surfaces functionalization that exists in the literature.[46,47] Furthermore, it offers the possibility to control oxygen evolution at the molecular level through the molecular catalyst function and catalyst activity. Our first generation system was based on a dinuclear manganese catalyst.[45] Designed as a functional model for Mn–catalase enzymes,[48–50] ligand **1**,[45,51] bearing a phenol, a tertiary amine and two pyridine binding sites was used to complex manganese. However, anchoring of our catalytic system on silica surfaces relied on the use of fragile imine linkers as well as the requiring the use of pre-functionalized silica particles (Scheme 2).

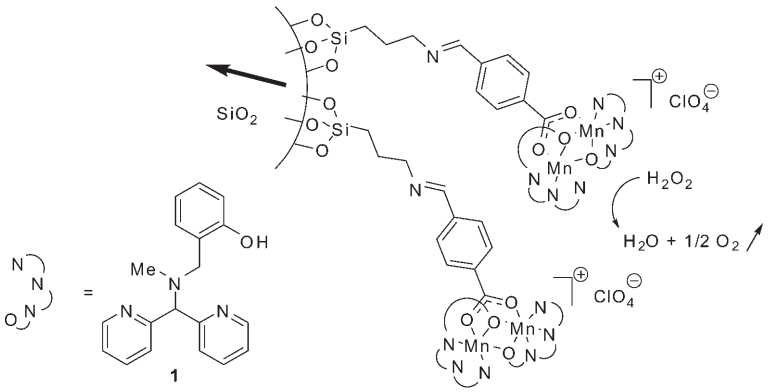


Scheme 2. Structure of surface bound synthetic dinuclear manganese complex as an immobilized catalase mimic.

Development of a general method for the functionalization of different non-functionalized surfaces with a stable synthetic catalytic motor would be of great interest. Here we report a general method for the functionalization of bare silica and glass microparticles with a synthetic manganese catalyst, through an amide or ether linkage, and the autonomous movement of these microscopic objects.

## Results and Discussion

The design of a molecular motor capable of generating kinetic energy from a chemical source comprises a linker between the object and the catalyst. As a first step towards a second-generation system and in order to increase the stability of our molecular system, we first designed a new amide-based tether.

Pre-functionalized aminopropyl silica microparticles **2** (40–63 μm) were modified to benzoic acid coated particles through the use of two different procedures. Acylation of primary amines using methyl 4-(chlorocarbonyl)benzoate,[52] followed by ester saponification afforded functionalized silica particles **3** (Scheme 3). The characteristic C=O absorption in IR at 1729 $cm^{-1}$ for ester functionalized particles and at 1680 $cm^{-1}$ for carboxylic acid groups was used to follow the functionalization. In a shorter process, direct coupling of terephthalic acid using DCC/DMAP also supplied the desired material, that showed carboxylic acid absorption in IR at 1682 $cm^{-1}$. Complexation with $Mn(ClO_4)_2$ in the presence of tetradentate ligand **1** and extensive washing of the microparticles to remove any unbound ligand or complex provided the silica particles functionalized with the dinuclear manganese catalyst **4**. The elaboration of surface bound manganese complexes was confirmed by IR spectroscopy and comparison with a non-bound manganese catalyst **5** synthesized from *p*-formylbenzoic acid.[45] Disappearance of the carboxylic acid band and appearance of the bridged carboxylate absorption in the 1590–1600 $cm^{-1}$ region was a strong indication that our manganese complex was covalently immobilized on the surface of the silica particles. Furthermore, the high activity for decomposition of $H_2O_2$ by these particles, using a 5% $H_2O_2$ solution in acetonitrile was also good evidence for the formation of the bound dinuclear manganese complex[53] (Scheme 3)

While using an excess of 4-(methoxycarbonyl)benzoic acid in the elaboration of functionalized particles **3**, a qualitative Kaiser test indicated the presence of free primary amino groups, as supported by the strong purple color observed.[54] Therefore a better description of the functionalized silica microparticles obtained via this procedure is depicted in Scheme 4 (method A).

The presence of reactive primary amino groups on the surface of the silica particles could perturb functionalization as well as characterization of more elaborated systems. In order to avoid the presence of free amine functionalities, we envisioned, as a key step towards our second generation system, an alternative approach using trialkoxy silanes, following a procedure by Jones.[55] Conceptually, the ligand for metal binding is first functionalized with the trialkoxy silane spacer which allows anchoring to the surface (Scheme 4, B). Moreover, this procedure should allow functionalization of bare materials, extending greatly the flexibility of our methodology. To enhance the robustness of the linkage between the particles and the molecular motor, increasing the stability of the system and avoiding plausible leakage of the manganese catalyst, we designed two new spacers based on the robust amide and ether links. To prevent competitive binding of the free carboxylic acid functionality to the silica surface, the methylester derivatives were used. Starting from terephthalic mono methyl ester **10**, condensation of corresponding acid chloride with 3-(triethoxysilyl)propan-1-amine afforded the amide tethered benzoic ester **11**. Alternatively, allylic ether **12** was converted into trimethoxy silane **13** via a

  

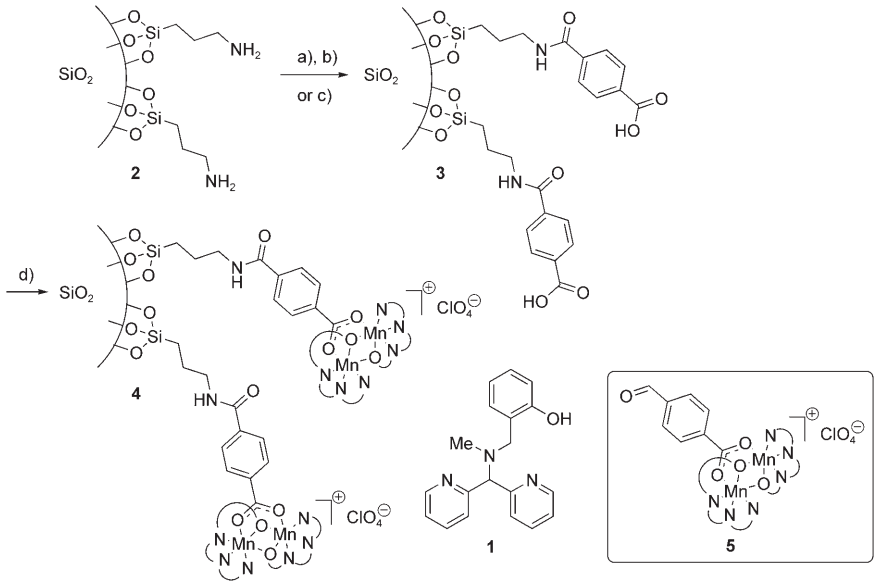

Scheme 3. Synthesis of surface bound manganese catalyst anchored via an amide linkage. a) Methyl 4-(chlorocarbonyl)benzoate, $Et_3N$, toluene; b) KOH, $H_2O$, EtOH; terephthalic acid, DCC, DMAP, toluene; d) $Mn(ClO_4)_2$, $Et_3N$, **1**, MeOH, MeCN.

Bare silica microparticles were then functionalized through their suspension in a solution of trialkoxy silane derivative in toluene, using either the amide **11** or the aromatic ether **13**. As expected, the Kaiser test revealed the absence of free amino groups on the surface of particles derivatized with **11** or **13** as the suspension remained yellow. Hydrolysis of ester moieties to reveal the free carboxylic acid groups, followed by complexation with $Mn(ClO_4)_2$ in presence of ligand **1**, produced dinuclear manganese catalyst functionalized particles **16** and **17** (Scheme 6).

The presence of the manganese complex on the surface of **16** and **17** was confirmed by IR

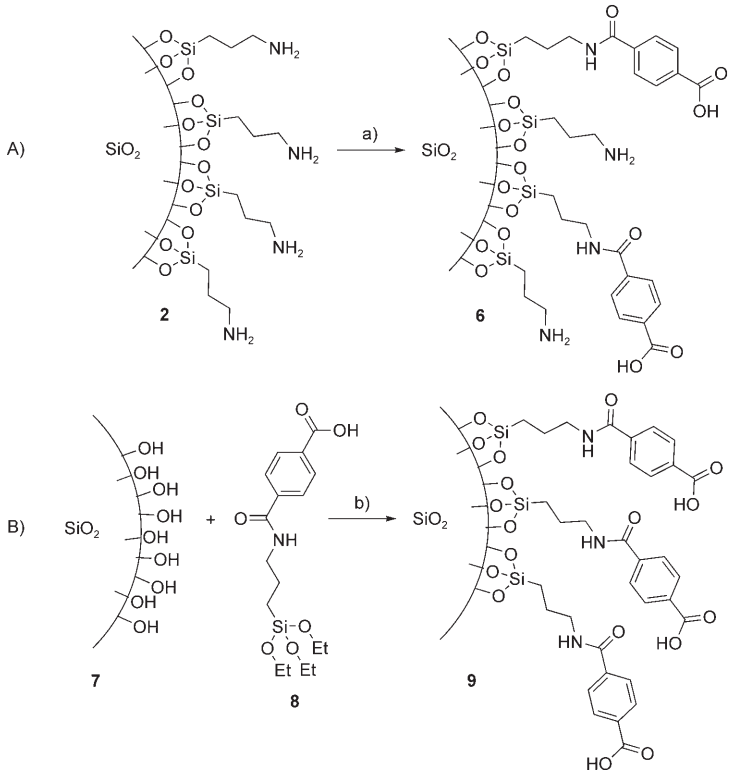

Scheme 4. Two different approaches allowing functionalization of silica particles: method A: Anchoring of benzoic acid moiety to amine functionalized silica; method B: Attachment of trialkoxysilane functionalized acid. a) Terephthalic acid, DCC, DMAO, toluene; b) $CHCl_3$, Δ.

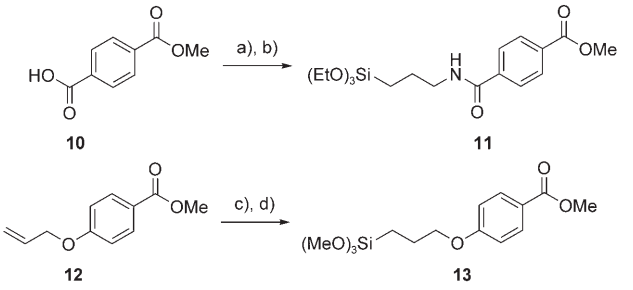

Scheme 5. Preparation of trialkoxy silane linkers. a) $SOCl_2$; b) 3-(triethoxysilyl)propan-1-amine, $Et_3N$, DCM, 95%; c) $HSiCl_3$, $H_2PtCl_6$, THF; d) MeOH, $Et_3N$, 65%.

platinum-catalyzed hydrosilylation reaction with $HSiCl_3$ followed by methanolysis[56] (Scheme 5).

spectroscopy, diffuse reflectance UV/Vis spectroscopy (Figure 1), EPR spectroscopy (Figure 2) and by elementary analysis. In the IR spectroscopy, as previously observed, disappearance of the carboxylic acid band and appearance of the bridged carboxylate absorption in the 1590–1600 $cm^{-1}$ region was a strong indication that our manganese complex was covalently immobilized on the surface of the silica particles. The presence of the dinuclear manganese catalyst was also confirmed by UV/Vis spectroscopy, as exemplified for the functionalized particles **16**. Comparison of the spectrum of the non-bound reference manganese catalyst **5** and the spectrum of the silica supported manganese catalyst **16**, obtained by diffuse reflectance UV/Vis, revealed the same characteristic absorption bands, at 222 nm, in the region between 245 and 275 nm and in the region between 285 and 295 nm. The stronger absorption for the silica-tethered manganese catalyst **16** around 243 nm was attributed to the structure of the amide benzoic ester linker, as supported by

  

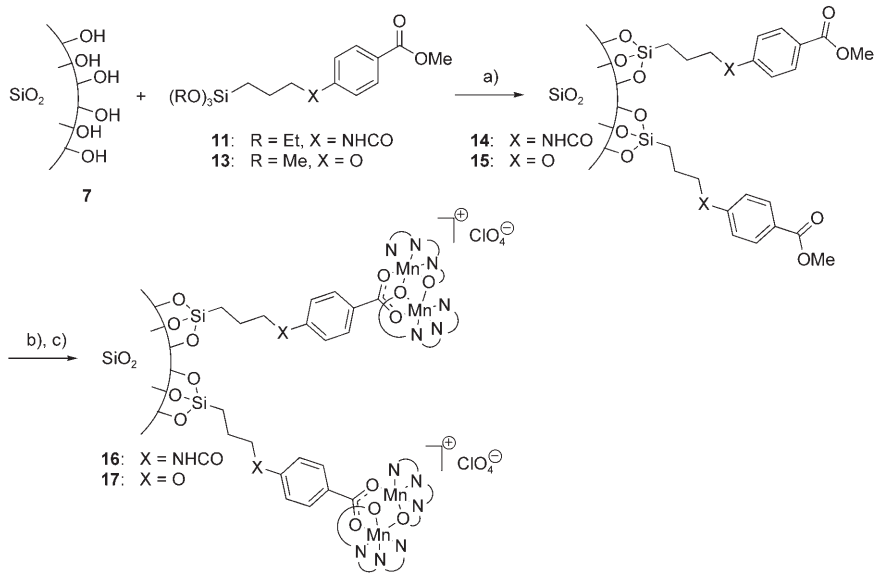


Scheme 6. Functionalization of bare silica microparticles with the dinuclear manganese catalyst. a) Toluene; b) KOH, $H_2O$, EtOH; $Mn(ClO_4)_2$, $Et_3N$, **1**, MeOH, MeCN.

the spectrum of the triethoxysilane derivative **11**, which shows a maximum absorption at 238 nm (Figure 1).

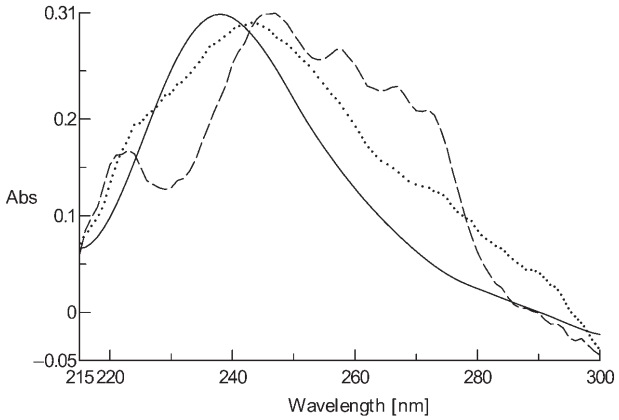


Figure 1. UV/Vis spectra of ——: amide tethered benzoic ester **11** ($2.10^{-5}$ M in $CH_3CN$), -----: non-bound manganese catalyst **5** ($2.10^{-5}$ M in $CH_3CN$) and •••••: silica supported manganese catalyst **16** (DR UV/Vis, suspension in glycerol).

EPR spectroscopy presents a powerful tool in the study of manganese-based catalytic systems. The EPR spectrum of ligand free silica supported $Mn^{II}$[57] is characteristic for a mononuclear quasi-octahedral $Mn^{II}$ species, which do not show discernible hyperfine splitting. The EPR spectra of both non-bound manganese catalyst **5** and silica supported manganese catalyst **16** bear a remarkable similarity to that of the dinuclear manganese(II) hydroxylation and epoxidation catalysts previously reported by our group.[58] These data strongly support the presence of the dinuclear manganese(II) catalyst on the surface of the silica particles **16**. As a control the EPR spectrum (Figure 2) of a ligand free silica supported mononuclear $Mn^{II}$ species confirms that non-ligated manganese is not involved to a significant extent in the catalase activity of the silica particles **16**. Indeed addition of $H_2O_2$ to $Mn^{II}$ modified particles (i.e., ligand free) results in immediate flocculation and precipitation as a brown inactive solid.

The manganese content of the immobilized dinuclear catalyst **16** was determined by ICP-AES to be 0.51% by mass, and hence the dinuclear catalyst loading was calculated to be about 0.05 mmol $g^{-1}$.

Decomposition of $H_2O_2$ as a solution in acetonitrile was observed for suspensions of both

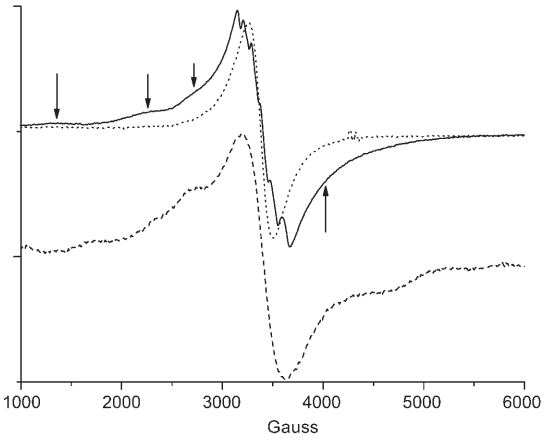


Figure 2. EPR spectra (X-band at 77 K) of ——: silica supported manganese catalyst **16** (suspension in DCM), -----: non-bound manganese catalyst **5** ($2.10^{-3}$ M in DCM) and •••••: ligand free silica supported $Mn^{II}$. Recording conditions: microwave power = 63.5 mW; modulation amplitude = 0.1 mT; modulation frequency = 50 kHz; time constant = 40.96 ms; $T$ = 77 K at 9.47 GHz.

materials (i.e., **16** and **17**). In order to study the movement induced by $O_2$ formation, a thin liquid film, containing a dilute suspension (in $CH_3CN$) of the functionalized microparticles **16** or **17**, mixed with non-functionalized microparticles (40–63 μm) as reference, on a microscope slide, was monitored after addition of a 5% $H_2O_2$ solution in $CH_3CN$. Oxygen evolution was observed as small oxygen bubbles appearing only on the catalyst-functionalized microparticles. Translational movement of the functionalized silica particles were observed (Figure 3; see also movie in the Supporting Information).

  

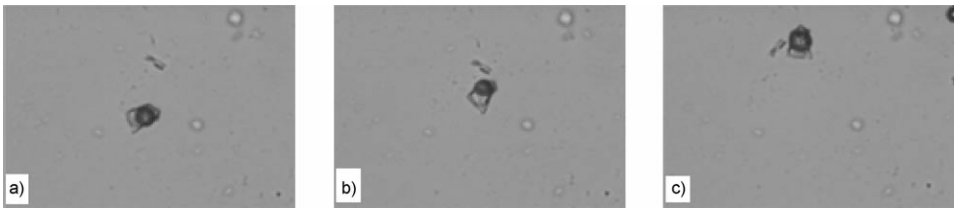


Figure 3. Translational movement of a catalyst-functionalized silica microparticle **17** at a) 0 s, b) 8 s, c) 19 s (average speed = 9.7 μm s$^{-1}$). Dimension of the video frame is 500 × 360 μm.

This successful method for functionalization of silica surfaces with the catalyst system encouraged us to the preparation of other functionalized surfaces. In order to induce autonomous movement of different micro-objects and to show the generality of our second generation molecular approach, we selected glass surfaces, giving that their functionalization with trialkoxy silane derivatives is also known.[59,60] Prior to functionalization, glass slides (0.5 × 0.5 cm) were activated using the method described by Linker.[61] Activated glass slides **18** were then coated via the condensation of trimethoxysilane **13**. Hydrolysis of the ester moiety and synthesis of the manganese catalyst were then performed as previously described (Scheme 7). Functionalization of the surface was monitored by contact angle measurements, which changed from 78–80° for ester functionalized glass slides to 55–60° for the more hydrophilic carboxylic acid functionalized glass slides and to 70–73° for the glass slides bearing the manganese catalyst **19**. Moreover, under microscope, glass slides were shown to be catalytically active in the decomposition of a 5% $H_2O_2$ solution in acetonitrile, giving us a good evidence for the covalent immobilization of the manganese complex. However, the glass slides were not suitable for movement in a thin liquid film, because of their large size. Nevertheless, glass fibers (glasswool, 10–25 μm in diameter), functionalized in the same manner, showed translational movement upon addition of aqueous $H_2O_2$ solution to a fibers suspension in acetonitrile (Figure 4; see also movie in the Supporting Information).

## Conclusion

In conclusion, we have developed a general method for easy functionalization of bare silica and glass surfaces with a synthetic manganese catalyst. Decomposition of $H_2O_2$ by this dinuclear metallic center into $H_2O$ and $O_2$ induced autonomous movement of silica microparticles and glass micro-sized fibers. Although several mechanisms have been proposed to rationalise movement of particles driven by $H_2O_2$ decomposition to $O_2$ and water (recoil from $O_2$ bubbles,[36,45] interfacial tension gradient[37–42]), it is apparent in the present system that ballistic movement is due to the growth of $O_2$ bubbles. The exact mechanism by which propulsion of the particles takes place in terms of the dependence of bubble formation on catalyst distribution and the presence of bubble nucleation sites is at present under further investigation. Future work will focus on the application of the methodology described here to achieve movement of nano-sized objects.

## Experimental Section

**General methods**: Chemicals were purchased from Acros, Aldrich, Fluka or Merck. Solvents for extractions and chromatography were technical grade. All solvents used in reactions, were freshly distilled from appropriate drying agents before use. Flash chromatography was carried out using

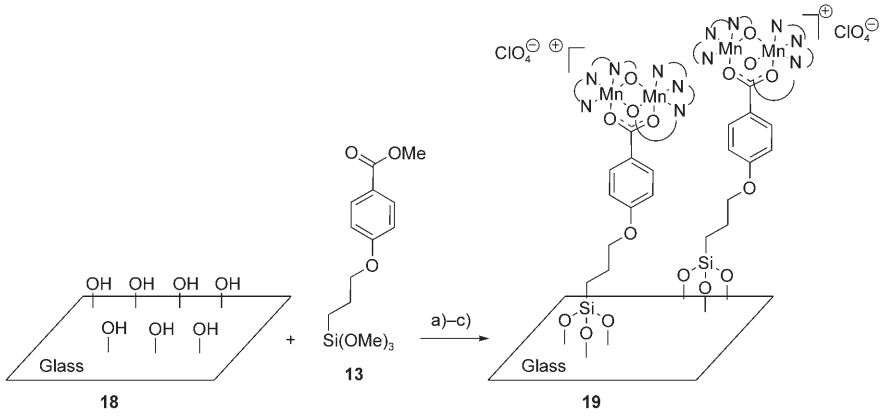


Scheme 7. Functionalization of bare glass surfaces. a) Toluene; b) KOH, $H_2O$, EtOH; c) $Mn(ClO_4)_2$, $Et_3N$, **1**, MeOH, MeCN.

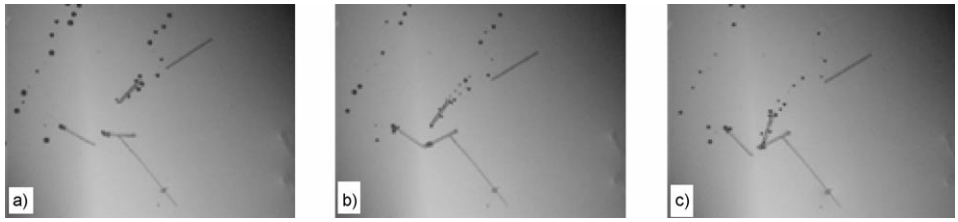


Figure 4. Translational movement of glass fibers **19** at a) 0 s, b) 65 s, c) 145 s (average speed = 1.6 μm s$^{-1}$). Dimension of the video frame is 1000 × 720 μm.

  

Merck silica gel 60 (230–400 mesh ASTM). NMR spectra were obtained using a Varian Gemini-400. Chemical shifts are reported in $\delta$ units (ppm) relative to the signal of TMS. MS(EI) spectra were obtained with a Jeol-600 spectrometer. FTIR spectra were recorded (as intimate mixtures with KBr) using a Nicolet Nexus FTIR spectrometer. EPR spectra (X-band, 9.46 GHz) were recorded in liquid nitrogen (77 K) on a Bruker ECS 106 instrument, equipped with a Bruker ECS 041 XK Microwave bridge and a Bruker ECS 080 magnet. Samples for measurement (250 μL) were transferred to an EPR tube, which was frozen in 77 K immediately. UV/Vis spectra were obtained using a diffuse reflectance attachment of a JASCO V-570 UV/Vis-NIR spectrophotometer. Images and movies of the moving particles and fibers were recorded using an Olympus BX 60 microscope, equipped with a Sony 3CCD DXC 950P digital camera, connected to a personal computer, using Matrox Inspector 2.1. imaging software. Contact angles were measured on a Krüss Drop Shape Analysis System DSA 10 Mk2.

**Kaiser test**: Three solutions were prepared: 1) 500 mg ninhydrin in 10 mL ethanol, 2) 80 g phenol in 20 mL ethanol, 3) 2 mL of an 1 mM aqueous solution of KCN diluted to 100 mL with pyridine. A small sample of the particles (2 to 5 mg) was placed in a test tube and three drops of each of the three reagents were added. The tube was heated at 100 °C for 2 min and the suspension turned purple (presence of free amino groups) or remained yellow (absence of free amino groups).

**Preparation of functionalized silica particles 4 according to Scheme 3**

Method A: 3-Aminopropyl functionalized silica gel **2** (400 mg, 40–63 μm, $\approx$1 mmol g$^{-1}$ $NH_2$ loading, Aldrich) was suspended in toluene (18 mL). 4-(Methoxycarbonyl)benzoic acid (500 mg, 2.77 mmol), DCC (573 mg, 2.77 mmol) and DMAP (34 mg, 0.28 mmol) were then added and the suspension was stirred at room temperature for 20 h. The silica microparticles were filtered off, washed with ethanol (3×20 mL) and with dichloromethane (3×10 mL) and dried in vacuo. IR (KBr): $\tilde{\nu}$=1729, 1591, 1548, 1403, 1284 cm$^{-1}$.

The samples were suspended in a mixture of ethanol and water (20 mL, 1:2 ratio). Potassium hydroxide (1.20 g) was added and the suspension was heated to reflux for 3 h. The silica particles were filtered off and washed with ethanol (3×30 mL) and dried in vacuo. IR (KBr): $\tilde{\nu}$=1680, 1579, 1508, 1369, 1085 cm$^{-1}$.

***Method B***: 3-Aminopropyl functionalized silica gel **2** (400 mg, 40–63 μm, $\approx$1 mmol g$^{-1}$ $NH_2$ loading, Aldrich) was suspended in toluene (12 mL). Terephthalic acid (100 mg, 0.60 mmol), DCC (124 mg, 0.60 mmol) and DMAP (10 mg, 0.08 mmol) were added and the suspension was stirred at room temperature for 17 h. The silica microparticles were filtered off, washed with ethanol (3×20 mL) followed by dichloromethane (3×10 mL) and dried in vacuo. IR (KBr): $\tilde{\nu}$ = 1682, 1575, 1511, 1372, 1087 cm$^{-1}$.

Manganese perchlorate hexahydrate (121 mg, 0.33 mmol) and ligand **1** (102 mg, 0.33 mmol) were dissolved in methanol (2 mL) and the solution was stirred for 30 min. The benzoic acid functionalized silica (200 mg) was then added and the mixture was stirred for 15 min before the addition of triethylamine (0.07 mL, 0.50 mmol). After an additional 15 min, acetonitrile (3 mL) was added and the mixture was left overnight. The solid was then collected by filtration and subsequently washed with methanol (3×5 mL) and acetonitrile (3×5 mL) and dried in vacuo. IR (KBr): $\tilde{\nu}$ = 1562, 1502, 1446, 1376, 1096 cm$^{-1}$.

**Preparation of reference non-bound manganese catalyst 5 according to Scheme 3**

Manganese perchlorate hexahydrate (724 mg, 2.0 mmol) and ligand **1** (610 mg, 2.0 mmol) were dissolved in methanol (10 mL) and the mixture was stirred for 30 min. Subsequently, 4-carboxybenzaldehyde (150 mg, 1.0 mmol) was added. After all solids were dissolved, triethylamine was added (0.42 mL, 3.0 mmol) at once and the solution turned pale green. After stirring for about 5 min, a solid precipitated and stirring continued for another 5 min. The solution was heated until boiling and gradually 15 mL of $CH_3CN$ were added, while keeping the mixture boiling. After the last few mL of $CH_3CN$ were added, the solids suddenly dissolved and the solution was left overnight. The supernatant was removed and the pale green crystals were washed thrice with MeOH and thrice with $Et_2O$ and dried under vacuum. Yield: 590 mg (0.61 mmol, 61%); IR: $\tilde{\nu}$ = 629, 760, 808, 883, 1014, 1097, 1159, 1203, 1276, 1403, 1454, 1483, 1558, 1602, 1660, 1760 cm$^{-1}$; ES-MS: *m*/*z*: 867.5 $[L_2Mn_2(O_2CC_6H_4CHO)]^+$; elemental analysis calcd (%) for $C_{46}H_{41}ClMn_2N_6O_9$: C 57.12, H 4.27, Cl 3.67, Mn 11.36, N 8.69, O 14.89; found: C 56.98, H 4.38, N 8.51.

***N*-(3-(Triethoxysilyl)propyl)-terephthalamic acid methyl ester 11**: Terephthalic acid mono methyl ester **10** (2.04 g, 11.2 mmol) was suspended in thionyl chloride (25 mL). The reaction mixture was heated under reflux for 3 h followed by removal of the excess thionyl chloride by distillation. The pale yellow solid obtained was used in the next step without further purification.

A solution of 3-(triethoxysilyl)propan-1-amine (2.01 g, 9.06 mmol) and triethylamine (1.37 g, 13.6 mmol) in dichloromethane (20 mL) were added to a solution of the acid chloride in dichloromethane (20 mL). The solution was refluxed for 1.5 h followed by concentration in vacuo. The crude reaction mixture was purified by column chromatography on silica gel (pentane/ethyl acetate 2:1) yielding trialkoxysilane **11** as a pale yellow solid (3.29 g, 10.7 mmol, 95%). $^1$H NMR (400 MHz, $CD_3Cl$, 25 °C): $\delta$=8.09 (d, *J*=8.1 Hz, 2H), 7.83 (d, *J*=8.1 Hz, 2H), 6.66 (s, 1H), 3.94 (s, 1H), 3.84 (q, *J*=6.9 Hz, 6H), 3.48 (dt, *J*=6.6, 6.6 Hz, 2H), 1.82–1.73 (m, 2H), 1.22 (t, *J*=6.9 Hz, 9H), 0.72 ppm (t, *J*=8.1 Hz, 2H); $^{13}$C NMR(100 MHz, $CD_3Cl$, 25 °C): $\delta$=166.6, 166.2, 132.3, 129.5, 129.4, 126.9, 58.4, 52.2, 42.3, 22.6, 18.1, 7.7 ppm; IR (KBr): $\tilde{\nu}$ = 3315, 2983, 2886, 1727, 1641, 1544, 1436, 1278, 1103, 1079 cm$^{-1}$; HRMS: *m*/*z*: calcd for $C_{18}H_{29}NO_6Si$: 383.1764, found: 383.1780.

**Methyl 4-(3-(trimethoxysilyl)propylcarbamoyl)benzoate (13)**: 4-Allyloxybenzoic acid methyl ester **12** (3.41 g, 17.8 mmol), trichlorosilane (3.61 g, 26.64 mmol) and hexachloroplatinic acid monohydrate (2 mg, 3.9 μmol) were added to dry THF (5 mL) and the mixture stirred at room temperature for 24 h. The solvent was then removed in vacuo and to the crude trichlorosilane adduct was added dropwise methanol/triethylamine 1:1 ((15 mL). The reaction mixture was stirred at room temperature for 2 h and subsequently diluted with diethyl ether (10 mL). The solvent were removed in vacuum and the crude reaction mixture was purified by column chromatography on silica gel (pentane/ethyl acetate 90:10) yielding trialkoxysilane **13** as a pale yellow solid (4.80 g, 15.3 mmol, 86%). $^1$H NMR(400 MHz, $CD_3Cl$, 25 °C): $\delta$=7.95 (dd, *J*=8.9, 2.1 Hz, 2H), 6.88 (dd, *J*=8.9, 2.1 Hz, 2H), 3.97 (td, *J*=6.5, 1.8 Hz, 2H), 3.86 (d, *J*=2.1 Hz, 3H), 3.57 (s, 9H), 1.93–1.82 (m, 2H), 0.77 ppm (td, *J*=8.1, 1.8 Hz, 2H); $^{13}$C NMR (100 MHz, $CD_3Cl$, 25 °C): $\delta$=166.9, 131.5, 122.4, 115.5, 114.1, 69.8, 51.8, 50.5, 22.5, 5.2 ppm; MS(EI): *m*/*z*: 314 (4), 272 (4), 241 (11), 152 (26), 121 (100), 93 (11), 91 (9), 65 (10); HRMS: *m*/*z*: calcd for $C_{14}H_{22}O_6Si$: 314.1185, found: 314.1191.

**Preparation of functionalized silica particles 16 and 17 according to Scheme 6**

***General procedure***: Merck silica gel 60 (400 mg, 230–400 mesh ASTM) was suspended in toluene (120 mL) and trialkoxysilane **11** or **13** (1.32 mmol) was added. The mixture was stirred at room temperature for 16 h then the silica microparticles were filtered off, washed with toluene (3×30 mL) and with ethyl acetate (3×30 mL) and dried in vacuo.

**Amide-functionalized particles (14)**: IR (KBr): $\tilde{\nu}$=1727, 1646, 1592, 1546, 1439, 1387, 1094 cm$^{-1}$.

**Ether-functionalized particles (15)**: IR (KBr): $\tilde{\nu}$=1716, 1608, 1513, 1438, 1105 cm$^{-1}$.

The microparticles were next suspended in a mixture of ethanol and water 1:3 (30 mL). Potassium hydroxide (1.10 g) was added to the suspension and the mixture was refluxed for 4 h. The silica particles were then filtered off and washed with water (3×20 mL) and ethanol (3×20 mL) and dried in vacuo.

**Amide-functionalized particles**: IR (KBr): $\tilde{\nu}$ = 1680, 1581, 1511, 1381, 1090 cm$^{-1}$.

**Ether-functionalized particles**: IR (KBr): $\tilde{\nu}$=1692, 1606, 1513, 1426, 1098 cm$^{-1}$.

Manganese perchlorate hexahydrate (121 mg, 0.33 mmol) and ligand **1** (102 mg, 0.33 mmol) were dissolved in methanol (2 mL) and the mixture was stirred for 30 min. The carboxylic acid functionalized silica (100 mg) was then added and the mixture was stirred 15 min before the addition of

  

triethylamine (0.07 mL, 0.50 mmol). After an additional 15 min, acetonitrile (3 mL) was added and the mixture was left overnight. The solid was then collected by filtration and was washed with methanol (3×5 mL) followed by acetonitrile (3×5 mL) and dried in vacuo.

**Amide-functionalized particles (16)**: IR (KBr): $\tilde{\nu}$ = 1598, 1561, 1481, 1376, 1096 $cm^{-1}$.

**Ether-functionalized particles (17)**: IR (KBr): $\tilde{\nu}$ = 1602, 1546, 1481, 1400, 1091 $cm^{-1}$.

**Preparation of functionalized glass slides and fibers 19**

***Glass activation***: Glass samples (10 slides or 500 mg fibers) were heated in a mixture of aqueous $NH_4OH$ (25% solution), aqueous $H_2O_2$ (30% solution) and water (50 mL, 1:1:2 ratio) for 3 h. The samples were then filtered off, rinsed with water (3×50 mL) and dried at 90°C for 3 h.

***Glass functionalization***: The activated glass samples **18** were suspended in toluene (200 mL) and trialkoxysilane **13** (500 mg, 1.59 mmol) was added. After stirring at room temperature for 14 h, the samples were filtered off, washed with toluene (3×30 mL) followed by ethyl acetate (3×30 mL) and dried in vacuo (water contact angle 78–80°).

The obtained samples were then suspended in a mixture of ethanol and water 1:3 (30 mL). Potassium hydroxide (1.50 g) was added and the suspension was heated to reflux for 3 h. The glass samples were filtered off and washed with ethanol (3×30 mL) and with water (3×30 mL) and dried at 90°C for 3 h (water contact angle 55–60°).

Manganese perchlorate hexahydrate (121 mg, 0.33 mmol) and ligand **1** (102 mg, 0.33 mmol) were dissolved in methanol (2 mL) and the mixture was stirred for 30 min. The glass samples were then added and the suspension was stirred 15 min before the addition of triethylamine (0.07 mL, 0.50 mmol). After an additional 15 min, the glass pieces were collected by filtration and were washed with methanol (3×5 mL) followed by acetonitrile (3×5 mL) and dried in vacuo (water contact angle 70–73°).

***Observation of autonomous movement***: A drop of a dilute suspension (≈1 mg in 5 mL $CH_3CN$) of the functionalized microparticles **19**, mixed with non-functionalized microparticles as reference was placed on a microscope glass slide. A drop of a 5% $H_2O_2$ solution in $CH_3CN$ was then added. Oxygen evolution was observed as small oxygen bubbles appearing on only the catalyst-functionalized microparticles. Typically, the movies of the movement of the particles were recorded after 5–10 min, after any perturbance due to the mixing processes were finished.

## Acknowledgements

This work was partially supported by the Deutsche Forschungsgemeinschaft (DFG) through a postdoctoral fellowship, by the Netherlands Organization for Scientific Research (NWO-CW) and by the National Research School Combination Catalysis (NRSC-C) through a postdoctoral fellowship.

[1] *Molecular Motors* (Ed.: M. Schliwa), Wiley-VCH, Weinheim, **2004**.
[2] E. M. Purcell, *Am. J. Phys.* **1977**, *45*, 3–11.
[3] A. Shapere, F. Wilczek, *Phys. Rev. Lett.* **1987**, *58*, 2051–2054.
[4] B. L. Feringa, R. A. van Delden, N. Koumura, E. M. Geertsema, *Chem. Rev.* **2000**, *100*, 1789–1816.
[5] B. L. Feringa, *Acc. Chem. Res.* **2001**, *34*, 504–513.
[6] L. E. Becker, S. A. Koehler, H. A. Stone, *J. Fluid Mech.* **2003**, *490*, 15–35.
[7] V. Balzani, M. Venturi, A. Credi, *Molecular Devices and Machines—A Journey into the Nanoworld*, Wiley-VCH, Weinheim, **2003**.
[8] R. A. van Delden, M. K. J. ter Wiel, N. Koumura, B. L. Feringa, *Molecular Motors* (Ed.: M. Schliwa), Wiley-VCH, Weinheim, **2004**, pp. 559–577.
[9] W. R. Browne, B. L. Feringa, *Nat. Nanotechnol.* **2006**, *1*, 25–35.
[10] Y. Shirai, J.-F. Morin, T. Sasaki, J. M. Guerrero, J. M. Tour, *Chem. Soc. Rev.* **2006**, *35*, 1043–1055.
[11] J.-F. Morin, Y. Shirai, J. M. Tour, *Org. Lett.* **2006**, *8*, 1713–1716.
[12] E. R. Kay, D. A. Leigh, F. Zerbetto, *Angew. Chem.* **2007**, *119*, 72–196; *Angew. Chem. Int. Ed.* **2007**, *46*, 72–191.
[13] A. R. Pease, J. O. Jeppesen, J. F. Stoddart, Y. Luo, C. P. Collier, J. R. Heath, *Acc. Chem. Res.* **2001**, *34*, 433–444.
[14] R. Ballardini, V. Balzani, A. Credi, M. T. Gandolfi, M. Venturi, *Acc. Chem. Res.* **2001**, *34*, 445–455.
[15] A. M. Brouwer, C. Frochot, F. G. Gatti, D. A. Leigh, L. Mottier, F. Paolucci, S. Roffia, G. W. H. Wurpel, *Science* **2001**, *291*, 2124–2128.
[16] D. A. Leigh, A. R. Thomson, *Org. Lett.* **2006**, *8*, 5377–5379.
[17] S. Saha, J. F. Stoddart, *Chem. Soc. Rev.* **2007**, *36*, 77–92.
[18] Z. Dominguez, T.-A. V. Khuong, H. Dang, C. N. Sanrame, J. E. Nuñez, M. A. Garcia-Garibay, *J. Am. Chem. Soc.* **2003**, *125*, 8827–8837.
[19] Y. Kuwatani, G. Yamamoto, M. Iyoda, *Org. Lett.* **2003**, *5*, 3371–3374.
[20] M. F. Hawthorne, J. I. Zink, J. M. Skelton, M. J. Bayer, C. Liu, E. Livshits, R. Baer, D. Neuhauser, *Science* **2004**, *303*, 1849–1851.
[21] G. S. Kottas, L. I. Clarke, D. Horinek, J. Michl, *Chem. Rev.* **2005**, *105*, 1281–1376.
[22] M. C. Jiménez, C. Dietrich-Buchecker, J.-P. Sauvage, *Angew. Chem.* **2000**, *112*, 3422–3425; *Angew. Chem. Int. Ed.* **2000**, *39*, 3284–3287.
[23] N. B. Holland, T. Hugel, G. Neuert, A. Cattani-Scholz, C. Renner, D. Oesterhelt, L. Moroder, M. Seitz, H. E. Gaub, *Macromolecules* **2003**, *36*, 2015–2023.
[24] Y. Liu, A. H. Flood, P. A. Bonvallet, S. A. Vignon, B. H. Northrop, H.-R. Tseng, J. O. Jeppesen, T. J. Huang, B. Brough, M. Baller, S. Magonov, S. D. Solares, W. A. Goddard, C.-M. Ho, J. F. Stoddart, *J. Am. Chem. Soc.* **2005**, *127*, 9745–9759.
[25] *Molecular Switches* (Ed.: B. L. Feringa), Wiley-VCH, Weinheim, **2001**.
[26] D. Gust, T. A. Moore, A. L. Moore, *Chem. Commun.* **2006**, 1169–1178.
[27] V. A. Azov, A. Beeby, M. Cacciarini, A. G. Cheetham, F. Diederich, M. Frei, J. K. Gimzewski, V. Gramlich, B. Hecht, B. Jaun, T. Latychevskaia, A. Lieb, Y. Lill, F. Marotti, A. Schlegel, R. R. Schlitter, P. J. Skinner, P. Seiler, Y. Yamakoshi, *Adv. Funct. Mater.* **2006**, *16*, 147–156.
[28] J. Areephong, W. R. Browne, N. Katsonis, B. L. Feringa, *Chem. Commun.* **2006**, 3930–3932.
[29] J. D. Badjic, V. Balzani, A. Credi, S. Silvi, J. F. Stoddart, *Science* **2004**, *303*, 1845–1849.
[30] J. D. Badjic, C. M. Ronconi, J. F. Stoddart, V. Balzani, S. Silvi, A. Credi, *J. Am. Chem. Soc.* **2006**, *128*, 1489–1499.
[31] T. R. Kelly, H. De Silva, R. A. Silva, *Nature* **1999**, *401*, 150–152.
[32] N. Koumura, R. W. J. Zijlstra, R. A. van Delden, N. Harada, B. L. Feringa, *Nature* **1999**, *401*, 152–155.
[33] D. A. Leigh, J. K. Y. Wong, F. Dehez, F. Zerbetto, *Nature* **2003**, *424*, 174–179.
[34] R. A. van Delden, M. K. J. ter Wiel, M. M. Pollard, J. Vicario, N. Koumura, B. L. Feringa, *Nature* **2005**, *437*, 1337–1340.
[35] M. M. Pollard, M. Lubomska, P. Rudolf, B. L. Feringa, *Angew. Chem.* **2007**, *119*, 1300–1302; *Angew. Chem. Int. Ed.* **2007**, *46*, 1278–1280.
[36] R. F. Ismagilov, A. Schwartz, N. Bowden, G. M. Whitesides, *Angew. Chem.* **2002**, *114*, 674–676; *Angew. Chem. Int. Ed.* **2002**, *41*, 652–654.
[37] W. F. Paxton, K. C. Kistler, C. C. Olmeda, A. Sen, S. K. St. Angelo, Y. Cao, T. E. Mallouk, P. E. Lammert, V. H. Crespi, *J. Am. Chem. Soc.* **2004**, *126*, 13424–13431.
[38] J. M. Catchmark, S. Subramanian, A. Sen, *Small* **2005**, *1*, 202–206.
[39] T. R. Kline, W. F. Paxton, T. E. Mallouk, A. Sen, *Angew. Chem.* **2005**, *117*, 754–756; *Angew. Chem. Int. Ed.* **2005**, *44*, 744–746.
[40] S. Fournier-Bidoz, A. C. Arsenault, I. Manners, G. A. Ozin, *Chem. Commun.* **2005**, 441–443.
[41] P. Dhar, T. M. Fischer, Y. Wang, T. E. Mallouk, W. F. Paxton, A. Sen, *Nano Lett.* **2006**, *6*, 66–72.
[42] Y. Wang, R. M. Hernandez, D. J. Bartlett, Jr., J. M. Bingham, T. R. Kline, A. Sen, T. E. Mallouk, *Langmuir* **2006**, *22*, 10451–10456.

  

[43] N. Mano, A. Heller, *J. Am. Chem. Soc.* **2005**, *127*, 11574–11575.
[44] S. T. Chang, V. N. Paunov, D. N. Petsev, O. D. Velev, *Nat. Mater.* **2007**, *6*, 235–240.
[45] J. Vicario, R. Eelkema, W. R. Browne, A. Meetsma, R. M. La Crois, B. L. Feringa, *Chem. Commun.* **2005**, 3936–3938.
[46] *Synthesis, Functionalization and Surface Treatment of Nanoparticles* (Ed.: M. I. Baraton), American Scientific Publishers, **2003**.
[47] *Chemistry of Nanomaterials: Synthesis, Properties and Applications* (Eds.: C. N. R. Rao, A. Müller, A.K. Cheetham), Wiley-VCH, Weinheim, **2004**.
[48] R. Hage, *Recl. Trav. Chim. Pays-Bas* **1996**, *115*, 385–395.
[49] A. J. Wu, J. E. Penner-Hahn, V. L. Pecoraro, *Chem. Rev.* **2004**, *104*, 903–938.
[50] J. W. de Boer, W. R. Browne, B. L. Feringa, R. Hage, *C. R. Chimie* **2007**, *10*, 341–354.
[51] J. Brinksman, R. La Crois, B. L. Feringa, M. I. Donnoli, C. Rosini, *Tetrahedron Lett.* **2001**, *42*, 4049–4052.
[52] A. Konosonoks, P. J. Wright, M.-L. Tsao, J. Pika, K. Novak, S. M. Mandel, J. A. Krause Bauer, C. Bohne, A. D. Gudmundsdóttir, *J. Org. Chem.* **2005**, *70*, 2763–2770.
[53] In a typical experiment, ≈1 mg of functionalized particles is suspended into 1 mL of acetonitrile then 1 drop of $H_2O_2$ solution (30% in $H_2O$) is added. Strong $O_2$ evolution is characteristic for the presence of manganese-based catalyst.
[54] E. Kaiser, R. L. Colescott, C. D. Bossinger, P. I. Cook, *Anal. Biochem.* **1970**, *34*, 595–598.
[55] K. Yu, C. W. Jones, *Organometallics* **2003**, *22*, 2571–2580.
[56] E. Lindner, T. Salesch, *J. Organomet. Chem.* **2001**, *628*, 151–154.
[57] Prepared as silica supported dinuclear manganese catalyst **16** but without the use of tetradentate ligand **1** in the last step.
[58] J. W. de Boer, W. R. Browne, J. Brinksma, P. L. Alsters, R. Hage, B. L. Feringa, *Inorg. Chem.* **2007**, *46*, 6353–6372.
[59] J. W. Goodwin, R. S. Harbron, P. A. Reynolds, *Colloid Polym. Sci.* **1990**, *268*, 766–777.
[60] W. Guo, E. Ruckenstein, *J. Membr. Sci.* **2003**, *215*, 141–155.
[61] W. Fudickar, A. Fery, T. Linker, *J. Am. Chem. Soc.* **2005**, *127*, 9386–9387.

Received: August 7, 2007
Revised: November 14, 2007
Published online: February 7, 2008

  